

## Calculation of the beam field in the LCLS bunch length monitor

G. Stupakov, Y. Ding and Z. Huang  
Stanford Linear Accelerator Center, Stanford University, Stanford, CA 94309

### Abstract

Maintaining a stable bunch length and peak current is a critical step for the reliable operation of a SASE based x-ray source. In the LCLS, relative bunch length monitors (BLM) right after both bunch compressors are proposed based on the coherent radiation generated by the short electron bunch. Due to its diagnostic setup, the standard far field synchrotron radiation formula and well-developed numerical codes do not apply for the analysis of the BLM performance. In this paper, we develop a calculation procedure to take into account the near field effect, the effect of a short bending magnet, and the diffraction effect of the radiation transport optics. We find the frequency response of the BLM after the first LCLS bunch compressor and discuss its expected performance.

## 1 Introduction

Maintaining a stable bunch length and peak current is a critical step for the reliable operation of a SASE based x-ray source. In the LCLS, relative bunch length monitors (BLM) right after both bunch compressors are proposed based on the coherent radiation generated by the short electron bunch [1]. A similar diagnostic device is used in the operation of the DESY VUV-FEL (FLASH) [2].

In the previous calculations of the beam radiation [1] standard formulae for the synchrotron radiation in the far field were used. However, due to the close proximity of the reflecting mirror to the magnet, applicability of these formulae is not fully justifiable. An additional factor which complicates the radiation pattern is the short length of the magnet comparable to the formation length of the radiation with the wavelength of the order of the bunch length. To the authors' knowledge, the available computer codes for calculation of the beam radiation (*e.g.*, the Synchrotron Radiation Workshop [3]) cannot be used for our case because the beam passes through the hole in the mirror.

It is a goal of this paper to calculate the electromagnetic field of an electron bunch which takes into account the near field effect, the effect of a short bending magnet, and the diffraction of the radiation caused by reflection from the mirror. We find the energy spectrum intercepted by the mirror in the first LCLS bunch compressor (BC1). We carry out these calculation assuming radiation in free space and neglecting the effect on the radiation of the conducting walls of the vacuum chamber.

We use Gaussian units throughout this paper.

## 2 Formulation of the problem

A simplified layout of the problem is presented in Fig. 1. The beam passes through a short magnet (*e.g.*, the last dipole of the first LCLS bunch compressor or BC1) of length  $l_m$  with the bending radius  $\rho$  and propagates along a straight line. A reflective mirror of diameter  $D$  with a circular hole of diameter  $d$  is located at a distance  $L$  from the exit edge of the magnet. The mirror is tilted at  $45^\circ$  and sends the beam field to the detector at the right angle to the beam trajectory. To simplify the calculation we, however, assume that the mirror's plane is perpendicular to the beam orbit (that is, it reflects the radiation back toward the magnet) and calculate the fields incident on as well as reflected from the mirror. Such modification of the geometry does not loose any significant physical effects of the problem.

We carried out calculations in the frequency domain. To calculate the Fourier component at frequency  $\omega$  of the beam field on the surface of the mirror we used two approaches. In the first one, a standard expression for the electromagnetic

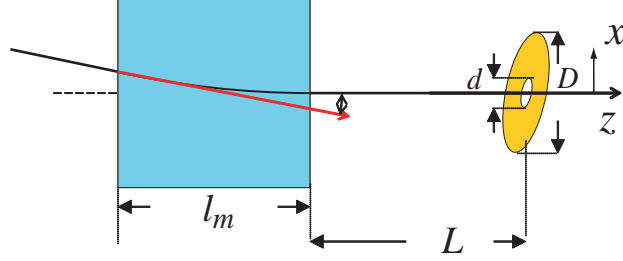


Figure 1: Layout of the bunch length monitor. The coordinate  $z$  is measured in the direction of beam propagation after the magnet with  $z = 0$  at the exit edge of the magnet. The coordinate  $x$  is in the plane of the orbit, and the coordinate  $y$  is perpendicular to the plane.

field of an electron moving in free space was used (see, *e.g.*, [4])

$$\begin{aligned} \mathbf{E}(\mathbf{r}, \omega) = & \frac{e}{\gamma^2} \int_{-\infty}^{\infty} dt \frac{\mathbf{n} - \boldsymbol{\beta}}{R^2(1 - \mathbf{n} \cdot \boldsymbol{\beta})^2} e^{i\omega(t+R/c)} \\ & + \frac{e}{c} \int_{-\infty}^{\infty} dt \frac{\mathbf{n} \times [(\mathbf{n} - \boldsymbol{\beta}) \times \dot{\boldsymbol{\beta}}]}{R(1 - \mathbf{n} \cdot \boldsymbol{\beta})^2} e^{i\omega(t+R/c)}. \end{aligned} \quad (1)$$

Here  $R$ ,  $\mathbf{n}$ ,  $\boldsymbol{\beta}$  and  $\dot{\boldsymbol{\beta}}$  are functions of time  $t$ :  $\mathbf{R}$  is the vector connecting the current position of the electron with the observation point  $\mathbf{r}$ , with  $R = |\mathbf{R}|$ ,  $\mathbf{n}$  is the unit vector directed along  $\mathbf{R}$ ,  $\boldsymbol{\beta}$  and  $\dot{\boldsymbol{\beta}}$  are the velocity and acceleration normalized by the speed of light, and  $\gamma = (1 - \beta^2)^{-1/2}$ . The first term in Eq. (1) is usually referred to as the *velocity field*. Note that for a relativistic particle with  $\gamma \gg 1$  the integrands in Eq. (1) have sharp narrow peaks in the direction for which  $\mathbf{n}$  is parallel to  $\boldsymbol{\beta}$  because in this direction the denominators  $(1 - \mathbf{n} \cdot \boldsymbol{\beta})^2 \sim 1/4\gamma^4$  become extremely small.

We remind the reader that the usual approximation for the *far zone* (FZ) is to neglect the velocity field and to take the limit  $R \rightarrow \infty$ :

$$\mathbf{E}_{\text{FZ}}(\mathbf{r}, \omega) \approx \frac{e}{cR} \int_{-\infty}^{\infty} dt \frac{\mathbf{n} \times [(\mathbf{n} - \boldsymbol{\beta}) \times \dot{\boldsymbol{\beta}}]}{(1 - \mathbf{n} \cdot \boldsymbol{\beta})^2} e^{i\omega(t+R/c)}.$$

In this expression, the value of  $R$  in front of the integral and the vector  $\mathbf{n}$  are considered as constant but  $R$  in the exponential (and of course  $\boldsymbol{\beta}$  and  $\dot{\boldsymbol{\beta}}$ ) are functions of time. If one integrates this expression over a finite time interval

from  $t_1$  to  $t_2$  the result is

$$\begin{aligned} \mathbf{E}_{\text{FZ}}(\mathbf{r}, \omega) = & -\frac{i e \omega}{c R} \int_{t_1}^{t_2} dt \mathbf{n} \times (\mathbf{n} \times \boldsymbol{\beta}) e^{i \omega(t+R/c)} \\ & + \frac{e}{c R} \frac{\mathbf{n} \times (\mathbf{n} \times \boldsymbol{\beta})}{1 - \mathbf{n} \cdot \boldsymbol{\beta}} e^{i \omega(t+R/c)} \Big|_{t_2} \\ & - \frac{e}{c R} \frac{\mathbf{n} \times (\mathbf{n} \times \boldsymbol{\beta})}{1 - \mathbf{n} \cdot \boldsymbol{\beta}} e^{i \omega(t+R/c)} \Big|_{t_1}. \end{aligned}$$

The last two terms are responsible for the *edge* radiation in the far zone [5].

We found advantageous for numerical calculations to use another expression for the electromagnetic field of a moving point charge [6]:

$$\mathbf{E}(\mathbf{r}, \omega) = \frac{i e \omega}{c} \int_{-\infty}^{\infty} \frac{dt}{R} [\boldsymbol{\beta} - \mathbf{n} (1 + i c / \omega R)] e^{i \omega(t+R/c)}. \quad (2)$$

This is the underlying equation used in the Synchrotron Radiation Workshop code [3]. Although this equation looks very different from Eq. (1), they give the same result for  $\mathbf{E}(\mathbf{r}, \omega)$ . The derivation of Eq. (2) using Lienard-Wiechert potentials is given in Appendix A. In passing, we note that neglecting the velocity field in Eq. (1) is not justified in our situations and yields very different numerical results as compared to Eq. (2).

To integrate Eq. (2) over the particle's orbit we split the integration path into three pieces. The first one is a straight line before the entrance to the magnet, the second one is an arc of a circular orbit inside the magnet, and the third one comprises the part of the trajectory after the exit from the magnet. The first two integrals were computed numerically using the Mathematica built in integration routine [7] (in the first integral the lower limit of integration  $-\infty$  was replaced by a large negative number). A direct numerical integration of the third integral turns out to be slow and poorly convergent because of a fast variation of the phase in the integrand. To improve the speed of calculation we used a method described in Appendix B, which is valid in the limit of large values of  $\gamma$ . Although formally the integration in Eq. (2) is extended beyond the position of the mirror, as is shown in Appendix B, the dominant contribution to the integral comes from the part of the trajectory located in front of the mirror.

### 3 Results of the calculations

The quantity  $c|E(\mathbf{r}, \omega)|^2/8\pi$  can be considered as an energy flow of the electromagnetic field. We calculated this quantity at the location of the mirror for various frequencies  $\omega$  and integrated it over the mirror surface. The resulting quantity is a measure of the energy reflected by the mirror in a unit interval of frequencies.

To illustrate the distribution of the spectral energy in the plane of the mirror, we plot in Fig. 2 the quantity  $|E|^2$  (in arbitrary units) in the mirror plane at

the distance  $L = 22$  cm for  $\omega/c = 50$  cm $^{-1}$ . We also assume that the  $\gamma$  factor for the beam is equal to 500, the bending radius of the magnet is 2.5 m, and the magnet length  $l_m = 22$  cm. The plot is truncated at small distances close

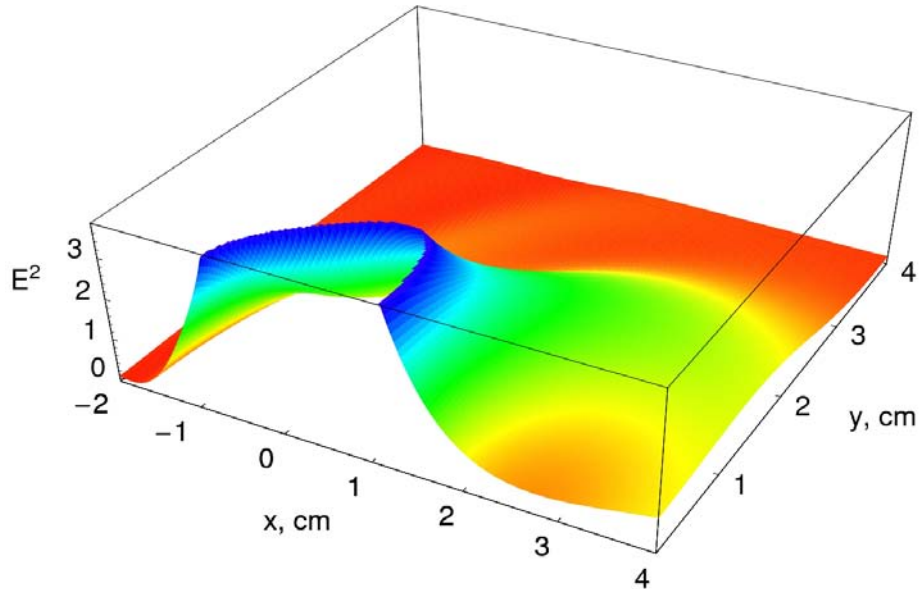


Figure 2: Square of the electric  $|E|^2$  (in arbitrary units) in the observation plane  $x, y$ . The picture is symmetric with respect to the axis  $x$ . The color coding goes from red through yellow, green, and blue as the intensity increases.

to the trajectory of the beam after the magnet ( $x = y = 0$ ) because the field has a singularity at the trajectory. Since the reflecting mirror has a hole for the passage of the beam, the field from this region is not reflected by the mirror.

Fig. 3 shows the same field as in Fig. 2 projected onto the surface of the mirror. The mirror outer diameter  $D = 7.6$  cm, and the diameter of the hole is  $d = 1.5$  cm. Note a complicated pattern of the field on the surface of the mirror.

We calculated the spectral energy  $S(k)$  intercepted by the mirror as a function of the wavenumber  $k = \omega/c$ ,  $S(k) \propto \int_{\text{mirror}} |E(\mathbf{r}, k/c)|^2 d^2r$ . It is normalized in such a way that the total energy reflected by the mirror due to the passage of a bunch with the longitudinal charge distribution  $\lambda(z)$  ( $\int \lambda(z) dz = 1$ ) is given by

$$\mathcal{E} = \int_0^\infty dk S(k) F(k), \quad (3)$$

where  $F(k)$  is the form factor related to the shape of the electron bunch,

$$F(k) = \left| \int_{-\infty}^\infty \lambda(z) e^{ikz} dz \right|^2. \quad (4)$$

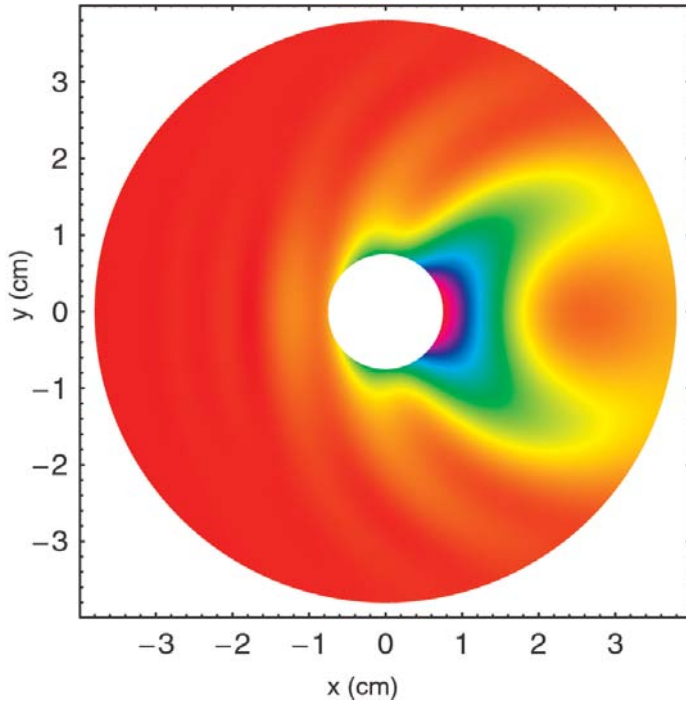


Figure 3: Distribution of the quantity  $|E|^2$  on the surface of a round mirror. Shown is a hole at the center of the mirror for the beam passage.

The plot of the function  $S(k)$  for the geometry of the mirror shown above is shown in Fig. 4.

Using the calculated spectrum we computed the amount of energy intercepted by the mirror for various values of the bunch lengths, taking a parabolic bunch profile that is expected after BC1 [1]. This energy as a function of the compressed rms bunch length is shown in Fig. 5.

## 4 Field reflected from the mirror

To calculate the field reflected from the mirror, we use the vectorial diffraction theory as the wavelengths of interests (comparable to the bunch length) are much smaller than the size of the mirror [4]. The detector is assumed to be located far away from the mirror. Although there may be additional optical elements between the mirror and the detector, we neglect them here in order to illustrate the calculation method. According to the diffraction theory, the detected field is given by

$$\mathbf{E}_r = \frac{ie^{ikR_1}}{2\pi R_1} \mathbf{k} \times \int_{\text{mirror}} (\mathbf{n}_1 \times \mathbf{E}_s) e^{-i\mathbf{k}\cdot\mathbf{r}} d^2r, \quad (5)$$

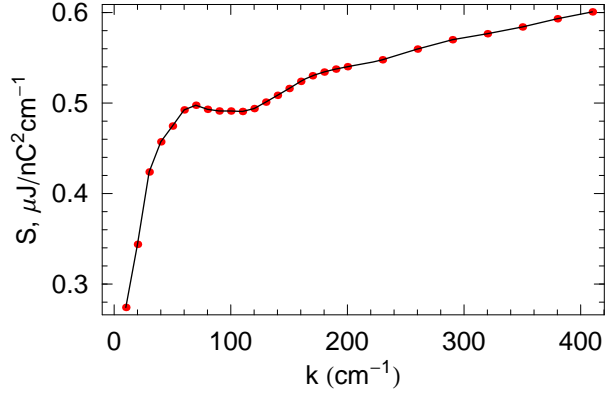


Figure 4: The spectral energy of the beam field intercepted by the mirror as a function of wavenumber  $k = \omega/c$ . The dots show the calculated values of  $S$ .

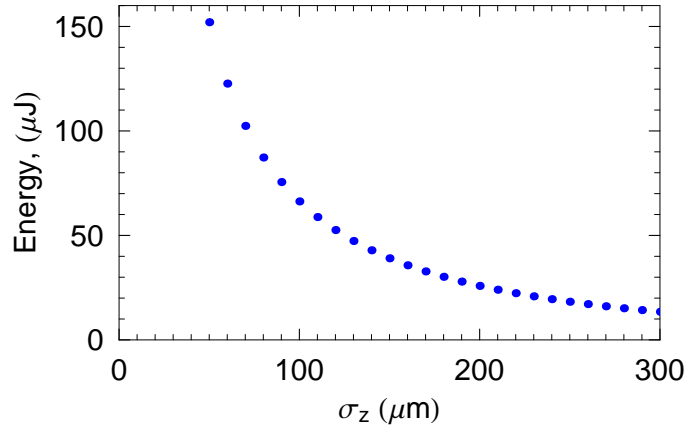


Figure 5: The reflected energy as a function of the compressed rms bunch length.

where  $R_1$  is the distance between the detector and the mirror,  $\mathbf{E}_s$  is the induced field at the mirror, and  $\mathbf{n}_1$  is the unit vector perpendicular to the mirror surface  $dS$ . The induced field is defined as follows. The total electric field on the surface of the mirror is the sum of the beam field  $\mathbf{E}$  (calculated in the previous section) and the induced field  $\mathbf{E}_s$ . Due to the boundary condition on the metal surface, the tangential component of this sum should vanish,  $\mathbf{n}_1 \times (\mathbf{E}_s + \mathbf{E})_{\text{mirror}} = 0$ , which gives

$$(\mathbf{n}_1 \times \mathbf{E}_s)_{\text{mirror}} = -(\mathbf{n}_1 \times \mathbf{E})_{\text{mirror}}. \quad (6)$$

We will make the small angle approximation around the field propagation direction (for the mirror perpendicular to the beam orbit, the reflected field propagates in the direction opposite to the  $z$  axis). Using the cylindrical coordinate system  $r$  and  $\phi$  in the mirror plane, we find the reflected field at the point with coordinates  $x$  and  $y$  in the detector plane as follows:

$$\mathbf{E}_r(x, y) = \frac{ik e^{ikR_1}}{2\pi R_1} \int_{d/2}^{D/2} r dr \int_0^{2\pi} d\phi \mathbf{E}^{\text{tang}} \exp \left[ -i \frac{kr}{R_1} (x \cos \phi + y \sin \phi) \right], \quad (7)$$

where the superscript “tang” indicates the component of the electric field tangent to the surface. Given the beam field  $\mathbf{E}$  on the mirror as found in the previous section, we integrated Eq. (7) numerically to compute the detected signal. As a numerical example, Fig. 6 shows the reflected field intensity distribution at the distance  $R_1 = 81$  cm from the mirror for  $\omega/c = k = 50$  cm $^{-1}$ . Note that the maximum of the field in the detector plane is shifted along the

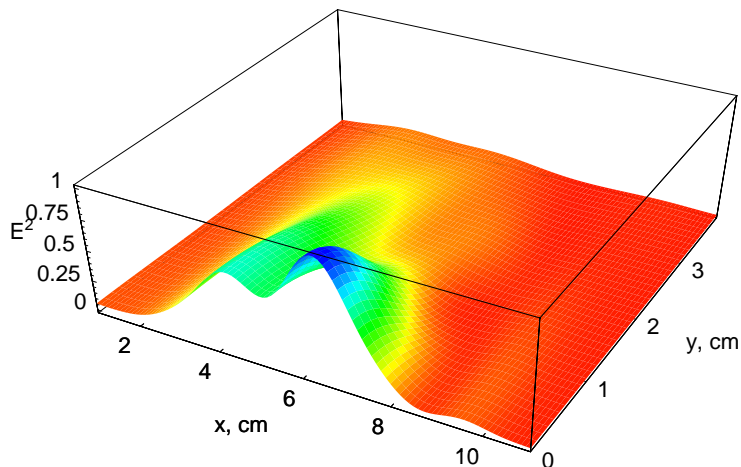


Figure 6: Square of the electric  $|E|^2$  (in arbitrary units) in the detector plane  $x, y$  located 81 cm away from the mirror. The plot is symmetric with respect to the  $x$  axis.

$x$  coordinate. Equation (7) can be generalized to include a paraboloid mirror that focuses the radiation.

## 5 Conclusion

We calculated the electromagnetic field intercepted and reflected by a metallic mirror for the geometry of the LCLS bunch length monitor. Unlike the previous calculations, we do not assume the far zone approximation for the radiation field. Our calculation takes into account the near field effect, the short length of the

bending magnet (the so called “edge radiation” effect), and the diffraction of the radiation caused by reflection from the mirror.

Our calculations assume propagation of the beam in free space and neglect the effect on the radiation of the conducting walls of the vacuum chamber. In reality, those effects are not negligible, and our result should be considered as an approximation to the real spectrum.

## 6 Acknowledgment

We wish to thank P. Emma, H. Loos, and J. Wu for useful discussions. This work was supported by Department of Energy contract No. DE-AC02-76SF00515.

## References

- [1] J. Wu, P. Emma, and Z. Huang, in *Proceedings of the 2005 Particle Accelerator Conference (2005)*, p. 428.
- [2] S. Casalbuoni, L. Fröhlich, O. Grimm, O. Peters, and J. Rossbach, in *Proceedings of the 2004 European Particle Accelerator Conference (2004)*, p. 2586.
- [3] O. Chubar and P. Elleaume, in *Proceedings of the 6th European Particle Accelerator Conference (1998)*, p. 1177.
- [4] J. D. Jackson, *Classical Electrodynamics* (Wiley, New York, 1999), 3rd ed.
- [5] R. A. Bosch, *Il Nuovo Cimento* **20 D**, 483 (1998).
- [6] O. V. Chubar, *Rev. Sci. Instrum.* **66 (2)**, 1872 (1995).
- [7] S. Wolfram, *The Mathematica Book* (Wolfram Media/Cambridge University Press, 1999), 4th ed.

## APPENDIX A

To derive Eq. (2) we use the Lienard-Wiechert potentials  $\mathbf{A}$  and  $\phi$ :

$$\mathbf{A}(\mathbf{r}, t) = \frac{e}{R} \frac{\boldsymbol{\beta}}{(1 - \mathbf{n} \cdot \boldsymbol{\beta})}, \quad \phi(\mathbf{r}, t) = \frac{e}{R} \frac{1}{(1 - \mathbf{n} \cdot \boldsymbol{\beta})}, \quad (\text{A1})$$

where the right hand side is evaluated at the retarded time  $t' = t - R/c$  [4]. The electromagnetic field in the time domain is given by

$$\mathbf{E}(\mathbf{r}, t) = -\frac{1}{c} \frac{\partial \mathbf{A}}{\partial t} - \nabla \phi. \quad (\text{A2})$$

If we substitute the Lienard-Wiechert potentials Eqs. (A1) into Eq. (A2) and then make the Fourier transform, we get the standard expression for the fields given by Eq. (1).

To obtain Eq. (2) we first make the Fourier transform of Eq. (A2):

$$\mathbf{E}(\mathbf{r}, \omega) = \int_{-\infty}^{\infty} \left( \frac{i\omega}{c} \mathbf{A} - \nabla\phi \right) e^{i\omega t} dt. \quad (\text{A3})$$

Using the retarded time  $t'$  as a new integration variable instead of  $t$ , with  $dt = (1 - \mathbf{n} \cdot \boldsymbol{\beta}) dt'$ , we find

$$\begin{aligned} \mathbf{E}(\mathbf{r}, \omega) &= \frac{i\epsilon\omega}{c} \int_{-\infty}^{\infty} dt' \frac{\boldsymbol{\beta}}{R} e^{i\omega(t'+R/c)} - e\nabla \int_{-\infty}^{\infty} dt' \frac{1}{R} e^{i\omega(t'+R/c)} \\ &= \frac{i\epsilon\omega}{c} \int_{-\infty}^{\infty} dt' \frac{\boldsymbol{\beta}}{R} e^{i\omega(t'+R/c)} + e \int_{-\infty}^{\infty} dt' \mathbf{n} \left( \frac{1}{R^2} - \frac{i\omega}{Rc} \right) e^{i\omega(t'+R/c)} \\ &= \frac{i\epsilon\omega}{c} \int_{-\infty}^{\infty} \frac{dt'}{R} \left[ \boldsymbol{\beta} - \mathbf{n} \left( 1 + \frac{ic}{\omega R} \right) \right] e^{i\omega(t'+R/c)}. \end{aligned}$$

Replacing the dummy integration variable  $t'$  with  $t$  this equation becomes Eq. (2).

## APPENDIX B

In this section we first show how to calculate the field of a relativistic charge moving along a straight line as shown in Fig. 7. We then use this result to simplify calculation of the contribution to the integral over the straight section of particle's orbit after the magnet.

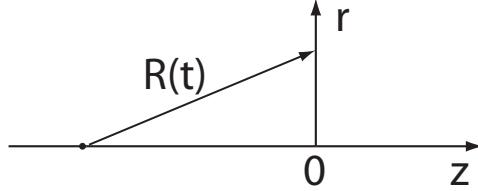


Figure 7: A relativistic particle is moving along a straight line  $x = y = 0$ . The field is calculated at a distance  $r$  from the orbit.

From Eq. (2), the radial component of the electric field  $E_r(\omega, r)$  at distance  $r$  from the particle's trajectory is given by

$$E_r(\omega, r) = -\frac{i\epsilon\omega r}{c} \int_{-\infty}^{\infty} \frac{dt}{R^2} \left( 1 + \frac{ic}{\omega R} \right) e^{i\omega(t+R/c)}, \quad (\text{B1})$$

where now  $R = r\sqrt{1 + \beta^2 c^2 t^2 / r^2}$ . Introducing the new variable  $\xi = ct/r$ , we write this integral in the following form

$$E_r(\omega, r) = -\frac{i e \omega}{c^2} \int_{-\infty}^{\infty} \frac{d\xi}{1 + \beta^2 \xi^2} \left( 1 + \frac{ic}{\omega r \sqrt{1 + \beta^2 \xi^2}} \right) \times \exp \left[ \frac{i \omega r}{c} \left( \xi + \sqrt{1 + \beta^2 \xi^2} \right) \right]. \quad (\text{B2})$$

Let us assume that  $\omega \gg c/r$  and neglect the second term in the bracket in front of the exponent. We also assume that  $\gamma \gg 1$  and the the main contribution to the integral comes from the negative values of  $\xi$  such that  $|\xi| \gg 1$ . Using expansion

$$\xi + \sqrt{1 + \beta^2 \xi^2} \approx \frac{\xi}{2\gamma^2} - \frac{1}{2\xi} \quad (\text{B3})$$

valid for large negative values of  $\xi$  and introducing the integration variable  $\tau = -\gamma/\xi$  we obtain

$$\begin{aligned} E_r(\omega, r) &\approx -\frac{i e \omega}{c^2} \int_{-\infty}^0 \frac{d\xi}{\xi^2} \exp \left[ \frac{i \omega r}{2c} \left( \xi/\gamma^2 - 1/\xi \right) \right] \\ &= -\frac{i e \omega}{\gamma c^2} \int_0^{\infty} d\tau \exp \left[ \frac{i \omega r}{2\gamma c} \left( \tau - 1/\tau \right) \right] \\ &= \frac{2e\omega}{\gamma c^2} K_1 \left( \frac{\omega r}{\gamma c} \right). \end{aligned} \quad (\text{B4})$$

This equation is a well known result for the Fourier image of the electric field of a relativistic charge moving with constant velocity [4].

It is important to emphasize here that in Eq. (B4) the integration over  $\xi$ , and hence time, goes from  $-\infty$  to 0. This means that in this approximation the contribution to the field comes only from the part of the trajectory before the observation point. In other words the field in the plane  $z = 0$  is not affected by the particle's motion behind the plane in which the observation point is located.

In our numerical calculation of the field due to the part of the trajectory behind the bending magnet we used Eq. (B1) with the lower limit  $t_1$  equal to 0 corresponding to the time of exiting from the magnet. We used the following symbolic relation to avoid integration behind the plane of the observation:

$$\int_{t_1}^{\infty} = \int_{-\infty}^{\infty} - \int_{-\infty}^{t_1} \approx \frac{2e\omega}{\gamma c^2} K_1 \left( \frac{\omega r}{\gamma c} \right) - \int_{-\infty}^{t_1}. \quad (\text{B5})$$

It turns out that the last integral in this equation is much easier to compute numerically than the original integral.